The Na^+/H^+ exchanger Nhx1p regulates the initiation of *Saccharomyces cerevisiae* vacuole fusion

Quan-Sheng Qiu[1,2] and Rutilio A. Fratti[1,*]

[1]Department of Biochemistry, University of Illinois at Urbana-Champaign, Urbana, IL 61801, USA
[2]School of Life Sciences, Lanzhou University, Lanzhou City, Tianshui Road 222, 730000, China
*Author for correspondence (rfratti@illinois.edu)

Accepted 28 June 2010
Journal of Cell Science 123, 3266-3275

doi:10.1242/jcs.067637

Summary

Nhx1p is a $Na^+(K^+)/H^+$ antiporter localized at the vacuolar membrane of the yeast *Saccharomyces cerevisiae*. Nhx1p regulates the acidification of cytosol and vacuole lumen, and is involved in membrane traffic from late endosomes to the vacuole. Deletion of the gene leads to aberrant vacuolar morphology and defective vacuolar protein sorting. These phenotypes are hallmarks of malfunctioning vacuole homeostasis and indicate that membrane fusion is probably altered. Here, we investigated the role of Nhx1p in the regulation of homotypic vacuole fusion. Vacuoles isolated from *nhx1*Δ yeast showed attenuated fusion. Assays configured to differentiate between the first round of fusion and ongoing rounds showed that *nhx1*Δ vacuoles were only defective in the first round of fusion, suggesting that Nhx1p regulates an early step in the pathway. Although fusion was impaired on *nhx1*Δ vacuoles, SNARE complex formation was indistinguishable from wild-type vacuoles. Fusion could be rescued by adding the soluble SNARE Vam7p. However, Vam7p only activated the first round of *nhx1*Δ vacuole fusion. Once fusion was initiated, *nhx1*Δ vacuoles appeared behave in a wild-type manner. Complementation studies showed that ion transport function was required for Nhx1p-mediated support of fusion. In addition, the weak base chloroquine restored *nhx1*Δ fusion to wild-type levels. Together, these data indicate that Nhx1p regulates the initiation of fusion by controlling vacuole lumen pH.

Key words: NHE1, SNARE, Vps44, Fusion, Vam7

Introduction

Membrane fusion of endosomal vesicles is crucial for maintaining cellular homeostasis in all eukaryotes. The machinery that controls membrane fusion is conserved from yeast to mammals (Jahn and Sudhof, 1999). We used vacuoles (lysosomes) from the yeast *Saccharomyces cerevisiae* to examine homotypic membrane fusion. Homotypic vacuole fusion requires soluble N-ethylmaleimide-sensitive factor (NSF) attachment protein receptors (SNAREs) and their chaperones Sec18p (NSF) and Sec17p (α-SNAP), the Rab GTPase Ypt7p and its effector homotypic fusion and vacuole protein sorting (HOPS) complex, Rho GTPase-regulated actin remodeling (Isgandarova et al., 2007) and a set of regulatory lipids that include ergosterol, diacylglycerol and phosphoinositides (Fratti et al., 2004; Jun et al., 2004; Kato and Wickner, 2001).

Membrane fusion occurs through distinct experimentally defined phases. During priming, Sec17p-bound cis-SNARE complexes are disassembled by Sec18p, releasing Sec17p (Mayer et al., 1996) and the soluble SNARE Vam7p (Boeddinghaus et al., 2002). Vam7p re-associates with vacuoles through its interactions with HOPS and phosphatidylinositol (PI) 3-phosphate (PI3P). After priming, vacuoles tether and dock in an Ypt7p-dependent cascade (Haas et al., 1995; Mayer and Wickner, 1997). During docking, SNARE complexes form in trans (between two membranes) (Ungermann et al., 1998), leading to the release of luminal calcium stores (Merz and Wickner, 2004a). Upon tethering and/or docking, vacuoles form three morphologically distinct domains. When vacuoles dock, they become tightly associated forming two flattened discs of apposed membranes termed the boundary. The perimeter of the boundary is the vertex ring and is enriched in proteins and lipids that catalyze fusion (Fratti et al., 2004; Wang et al., 2003; Wang et al., 2002). Fusion occurs at the vertex ring, resulting in the internalization of the boundary membranes as an inverted lumenal vesicle.

Ion homeostasis plays an important function in membrane trafficking. A wealth of research has been performed on understanding the roles of Ca^{2+} transport, as well as pH regulation by V-ATPases. However, the role of $Na^+(K^+)$ transporters in membrane traffic is not well understood. The yeast $Na^+(K^+)/H^+$ antiporter Nhx1p, originally identified as Vps44p, is homologous to the NHE family of transporters in mammalian cells. Nhx1p regulates vacuolar pH by transporting Na^+ and K^+ ions into the vacuole lumen while exporting H^+ into the cytoplasm (Brett et al., 2005). The exchange of $Na^+(K^+)$ and H^+ is associated with regulating the trafficking of cargo from late-endosomal compartments to the vacuole (Bowers et al., 2000). Nhx1p is a polytopic protein with 12 transmembrane domains that comprise the ion transporter, and an extended cytoplasmic C-terminal domain. Whereas the ion transporter domain is well conserved throughout the NHE family, the cytoplasmic tail is highly divergent and serves a multitude of functions that include interactions with calmodulin (Yamaguchi et al., 2005), ezrin (Wu et al., 2004) and phosphoinositides (Aharonovitz et al., 2000). The cytoplasmic tail of Nhx1p is glycosylated (Wells and Rao, 2001) and interacts with the GTPase activating protein (GAP) Gyp6p that can activate both Ypt6p and Ypt7p (Ali et al., 2004; Will and Gallwitz, 2001). Deletion of *NHX1* in *S. cerevisiae* leads to changes in vacuolar morphology, a vacuolar protein-sorting defect and the hyperacidification of the vacuole lumen (Bonangelino et al., 2002; Brett et al., 2005; Seeley et al., 2002).

In this study, we examined the role of Nhx1p in vacuole homotypic fusion. We found that vacuoles from *nhx1*Δ yeast are attenuated for fusion and that Nhx1p regulates the initiation of fusion. Furthermore, we found that the Nhx1p regulates fusion via ion transport and maintenance of vacuole pH.

Results

Nhx1p has been reported to operate in vesicle trafficking between pre-vacuolar late endosomes and the vacuole (Bowers et al., 2000; Nass and Rao, 1998). Owing to the reported altered vacuole morphology and defective protein sorting, we examined whether Nhx1p might play an important role in regulating vacuole fusion. To examine the vacuolar phenotype of our deletion strains, we incubated wild-type (WT) and *nhx1*Δ strains with the vital dye FM4-64, which collects in the vacuole (Vida and Emr, 1995). Previously, *nhx1*Δ strains were shown to have a Class E vacuolar compartment, meaning that cells harbored a single large vacuole, flanked by enlarged prevacuolar compartments (PVC) (Bowers et al., 2000; Seeley et al., 2002). As expected, Class E compartments were observed; however, we also observed an increase in cells harboring multiple vacuoles (Fig. 1A). When quantitated, there was a 50% reduction in cells harboring a single vacuole (Fig. 1B). Concomitantly, there was a several-fold increase in cells with multiple vacuoles, suggesting that vacuole fusion was probably impaired in vivo. To determine whether vacuoles from *nhx1*Δ yeast contained the necessary components for homotypic fusion, western blot analysis was performed. No significant differences were observed in the composition of the fusion machinery on mutant vacuoles relative to their isogenic WT counterparts (Fig. 1C). Vam3p and Vam7p levels were slightly reduced on *nhx1*Δ vacuoles relative to WT. Vph1p levels were also reduced on *nhx1*Δ vacuoles (~50%) relative to WT vacuoles (Fig. 1C). This is consistent with a previous finding that showed reduced vacuole-localized Vph1p in *nhx1*Δ cells (Bowers et al., 2000). To document the presence of Nhx1p on purified vacuoles, we constructed a strain harboring Nhx1p-GST. Vacuoles were isolated from the WT and Nhx1p-GST strains and examined by western blot. We found that Nhx1p-GST was indeed enriched on vacuoles relative to the microsomal fraction (Fig. 2A). We also blotted for endosomal proteins that do not cycle between endosomes and the vacuole. In Fig. 2A, we observed that the ESCRT I protein Vps23p (Katzmann et al., 2001) and the ESCRT III component Snf7p (Babst et al., 2002) were enriched in the microsomal fraction and only lightly detectable in the vacuole fraction. By contrast, the vacuolar GTPase Ypt7p was highly enriched on vacuoles relative to bulk microsomes. This suggests that although vacuoles do co-purify with trace levels of endosomal contaminants, the high levels of Nhx1-GST on vacuoles was not due to contamination. The detection of robust Nhx1p-GST levels in vacuole preparations suggests that a significant fraction of the antiporter is always present on the vacuole membrane. To further document the distribution of Nhx1p, we constructed a strain of yeast harboring an Nhx1p-GFP fusion protein. In Fig. 2B, we show a single slice from a deconvolved *z*-stack of images of a vacuole harboring Nhx1p-GFP stained with PSS-380 to label phosphatidylserine. Here we found that Nhx1p-GFP was indeed on the limiting membrane of the vacuole and not on a neighboring endosomal vesicle. Although PVC membranes contain high

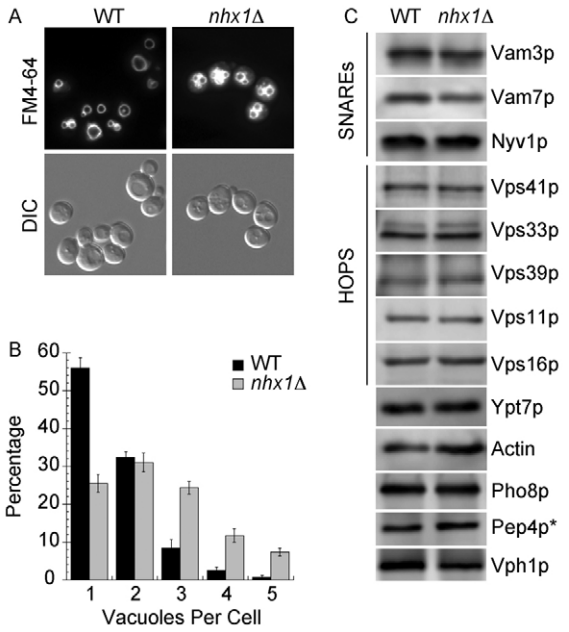

Fig. 1. Deletion of *NHX1* causes vacuole fragmentation. (**A**) Wild-type and *nhx1*Δ yeast cells were incubated with 5 µM FM4-64 to label vacuoles. Cells were washed with PBS and mounted in agarose for microscopy. Cells were photographed using DIC, and FM4-64 images were acquired using a 43 HE CY 3 shift-free filter set. (**B**) Quantification of the number of vacuoles per cell in WT BJ3505 and RFY5 (BJ3505 *nhx1*Δ) yeast. (**C**) Analysis of core fusion components. Vacuoles were isolated from WT BJ3505 and RFY5 cells. Membranes (5 µg) were mixed with 2× loading buffer, resolved by SDS-PAGE and transferred to nitrocellulose. Western blots were performed with indicated antibodies and bands were detected using enhanced chemifluorescence and a Storm Phosphorimager. *To examine the effect of deleting *NHX1* on Pep4p trafficking, vacuoles were examined from DKY6281 and RFY6 (DKY6281 *nhx1*Δ).

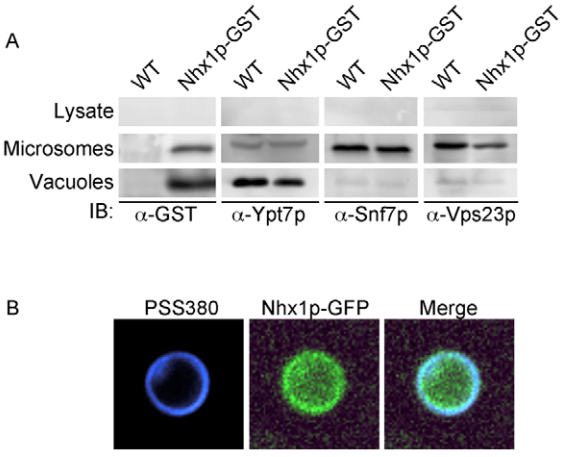

Fig. 2. Vacuole localization of Nhx1p. (**A**) Samples were isolated from WT DKY6281 and RFY9 (Nhx1p-GST) strains. Western blots were performed on whole cell lysate, a microsomal fraction and purified vacuoles. Each lane contained 10 µg of protein for lysate and microsome samples. Microsomes and lysates were prepared as described elsewhere (Sorin et al., 1997). Vacuole lanes contained 5 µg of protein. Antibody against GST was used to detect Nhx1p-GST, and anti-Ypt7p was used to detect the vacuolar GTPase. Antibodies against Vps23p and Snf7p were used to detect early endosomal proteins. (**B**) Vacuoles harboring Nhx1p-GFP were used for fluorescence microscopy. Phosphatidylserine was stained with 2.5 µM PSS-380. A *z*-stack of images was taken of vacuoles and deconvolved using AxioVison 3D deconvolution software. Shown is the center slice of a *z*-stack.

concentrations of Nhx1p, these results illustrate the unambiguous presence of Nhx1p-GFP on the vacuole membrane. In whole cells, PVC-localized Nhx1-GFP was sufficiently bright to obscure vacuole labeling and quantitation. However, when isolated vacuoles were quantitated, we found that 94.1% (±3.4 s.e.m., *n*=541 vacuoles) harbored visible Nhx1-GFP. This illustrates that vacuole localization is not atypical and that Nhx1 is normally part of the organelle composition.

We next examined the effect of Nhx1p on vacuole homotypic fusion. Fusion is measured by the maturation of proPho8p (pro-alkaline phosphatase) by the protease Pep4p. These experiments were carried out using the reciprocally deleted strains DKY6281 (*PEP4 pho8*Δ) and BJ3505 (*pep4*Δ *PHO8*) (Haas et al., 1994). We deleted *NHX1* from these strains to generate RFY5 and RFY6, and found that the fusion of *nhx1*Δ vacuoles was attenuated and showed an approximate 35% reduction in fusion relative to WT vacuoles (Fig. 3A). This was not due to altered trafficking of Pho8p or Pep4p (Fig. 1C). To investigate whether the difference was due to a kinetic defect, we employed a method shown to differentiate the first round of fusion from later ongoing rounds (Merz and Wickner, 2004b). Here we used an excess of reporter vacuoles (*PHO8 pep4*Δ) to report late rounds of fusion (Fig. 3B), or an excess of effector vacuoles (*pho8*Δ *PEP4*) to report early fusion (Fig. 3C). We found that *nhx1*Δ vacuoles were only defective in early rounds of fusion (Fig. 3C) and not later ongoing rounds (Fig. 3B). This

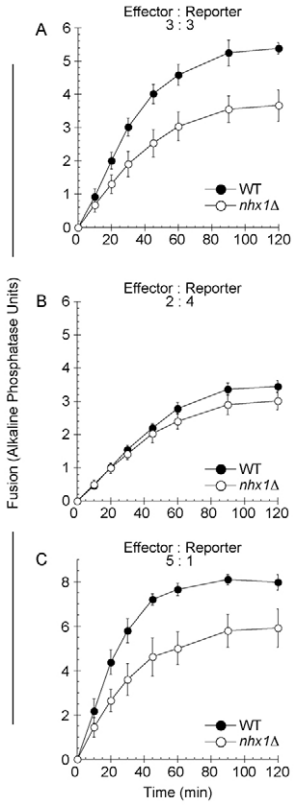

Fig. 3. Vacuoles from *nhx1*Δ yeast show a defect in early rounds of fusion. Vacuoles were harvested from wild-type (WT) and *nhx1*Δ yeast and tested for fusion. (**A**) Standard fusion reactions used equal amounts of reporter (3 μg *PHO8 pep4*Δ) and effector (3 μg *pho8*Δ *PEP4*) vacuoles. (**B**) To illustrate late rounds of vacuole fusion, an excess of reporter vacuoles (4 μg) was incubated with 2 μg of effector vacuoles. (**C**) An excess effector vacuoles (5 μg) was incubated with 1 μg of reporter vacuoles to monitor early rounds of fusion. Error bars represent s.e.m. (*n*=3).

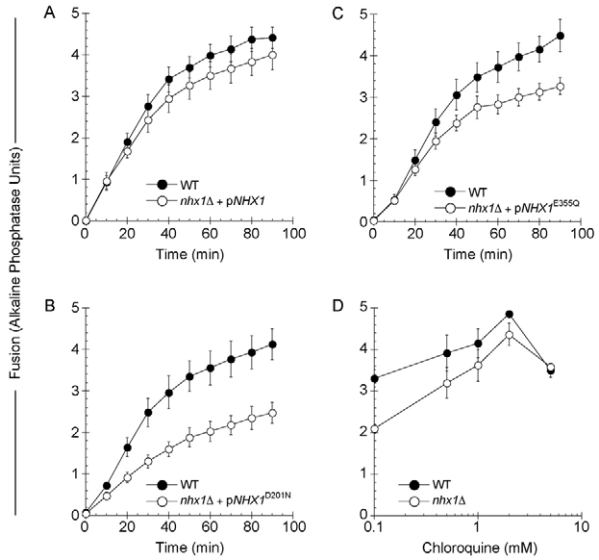

Fig. 4. Nhx1p ion transport is important for membrane fusion. Mutant *nhx1*Δ strains were complemented with WT *NHX1* (**A**) or the point mutants D201N (**B**) and E355Q (**C**). Independent 30 μl reactions were used for each timepoint. (**D**) WT and *nhx1*Δ vacuoles were treated with the weak base chloroquine at the indicated concentrations and examined for fusion. Error bars represent s.e.m. (*n*=3).

suggests that kinetics of early fusion stages are regulated in part by Nhx1p. Mutant *nhx1*Δ strains were complemented with WT or mutant *NHX1* encoded on pRS413 or pRS414. We found that strains complemented with WT *NXH1* were rescued and fused at WT levels, demonstrating that the Nhx1p is directly involved in fusion regulation (Fig. 4A). We also used mutations that have been previously characterized by Stevens and colleagues (Bowers et al., 2000). These mutations target conserved acidic residues required for ion transport in the NHE family (Dibrov et al., 1998; Fafournoux et al., 1994; Inoue et al., 1995). We found that Nhx1p^{D201N} did not restore fusion (Fig. 4B), which was consistent with previous findings showing that FM4-64 and CPY trafficking were not restored with Nhx1p^{D201N}. Interestingly, Nhx1p^{E355Q} was previously shown to fully complement FM4-64 and CPY trafficking (Bowers et al., 2000), yet this mutant only partially rescued fusion in our experiments (Fig. 4C). This is consistent with a previous report that showed a partial complementation of CPY trafficking and vacuolar pH by Nhx1p^{E355Q} (Mukherjee et al., 2006). These data indicate that ion transport activity is required for Nhx1p-mediated fusion regulation. To determine whether the acidified lumenal pH of *nhx1*Δ vacuoles caused the attenuated fusion, we treated WT and mutant vacuoles with the weak base chloroquine, a lysosomotropic agent that preferentially accumulates in lysosomes. We found that treating vacuoles with chloroquine restored *nhx1*Δ vacuole fusion to WT levels (Fig. 4D), further illustrating that Nhx1p regulates vacuole fusion by controlling lumenal pH.

Because *nhx1*Δ cells contain wild-type levels of the fusion machinery, we investigated whether we could bypass the fusion defect. To stimulate *nhx1*Δ vacuoles, we used recombinant Vam7p, which bypasses blocks in early fusion stages such as priming and Ypt7p-dependent tethering (Fratti et al., 2007; Thorngren et al., 2004). Here, WT and *nhx1*Δ vacuoles were treated with anti-Sec17p IgG to inhibit priming. Reactions were rescued with GST-Vam7p or GST-Vam7p^{Q283R}, which disrupts the 3Q:1R SNARE

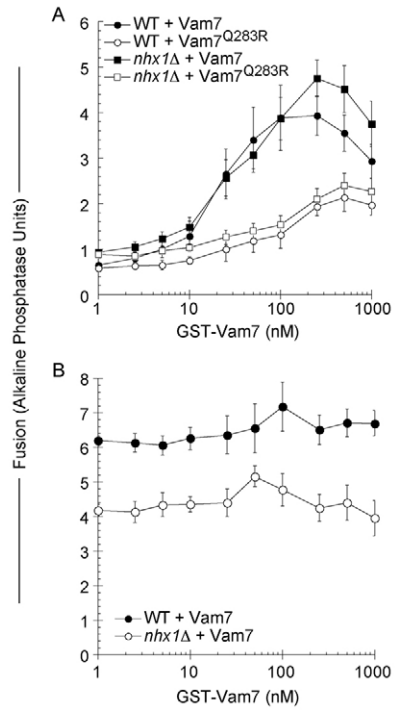

Fig. 5. Vam7p activates WT and *nhx1*Δ fusion when priming is blocked. (**A**) Fusion reactions using WT or *nhx1*Δ vacuoles were treated with anti-Sec17p IgG to block priming. Recombinant Vam7p (black symbols) and Vam7p^{Q283R} (white symbols) were added at the indicated concentrations to bypass anti-Sec17p. (**B**) WT and *nhx1*Δ vacuoles were incubated with recombinant Vam7p in the absence of inhibitors and tested for fusion. Error bars represent s.e.m. (*n*=3).

paradigm and does not support fusion under native membrane conditions (Fratti et al., 2007). Both WT and *nhx1*Δ vacuoles were rescued by Vam7p (Fig. 5A, black symbols). As one would predict, Vam7p^{Q283R} did not stimulate either set of vacuoles (Fig. 5A, white symbols). These data illustrate that mutant vacuoles have all the necessary components for full fusion, and that mis-sorted cargo (e.g. CPY) has no deleterious effect. Furthermore, this demonstrates that the Pho8p reporter system is not affected by the acidified lumen of *nhx1*Δ vacuoles. In separate experiments, we examined whether Vam7p could stimulate fusion when vacuoles were allowed to undergo priming. Uninhibited reactions were treated with Vam7p as described above and tested for fusion. We found that exogenous Vam7p did not increase the fusion of WT or *nhx1*Δ vacuoles (Fig. 5B). This is consistent with our previous report showing that exogenous Vam7p does not alter uninhibited fusion reactions (Fratti et al., 2007).

Exogenous Vam7p readily enters into complexes with endogenous SNAREs and HOPS. To verify whether Vam7p-dependent rescue of *nhx1*Δ vacuoles also requires these complexes, we performed GST-Vam7p pull-down assays. SNARE priming was inhibited with anti-Sec17 IgG. After 15 minutes, anti-Vam3p was added to the indicated reactions and allowed to act for 5 minutes. Fusion reactions were then rescued with 400 nM GST-Vam7p and incubated for an additional 70 minutes (Fig. 6A). In agreement with the findings in Fig. 5A, fusion was restored when either WT or mutant vacuoles were treated with Vam7p (Fig. 6B). GST-Vam7p complexes were isolated and examined by western blotting. GST-Vam7p complexes included the SNAREs Vam3p and Nyv1p, and the HOPS subunits Vps16p and Vps33p (Fig. 6C). SNARE complex formation was blocked when reactions were treated with anti-Vam3p. GST-Vam7p complexes were indistinguishable between WT and *nhx1*Δ vacuoles, suggesting that SNARE-HOPS complex formation was not inhibited by the lack of Nhx1p. The interaction between Vam7p and HOPS was not disrupted by anti-Vam3p, possibly owing to the direct interaction of the Vam7p Phox homology (PX) domain with HOPS (Stroupe et al., 2006).

As seen in Fig. 6, exogenous GST-Vam7p was able to form complexes with free SNAREs and HOPS on *nhx1*Δ vacuoles when

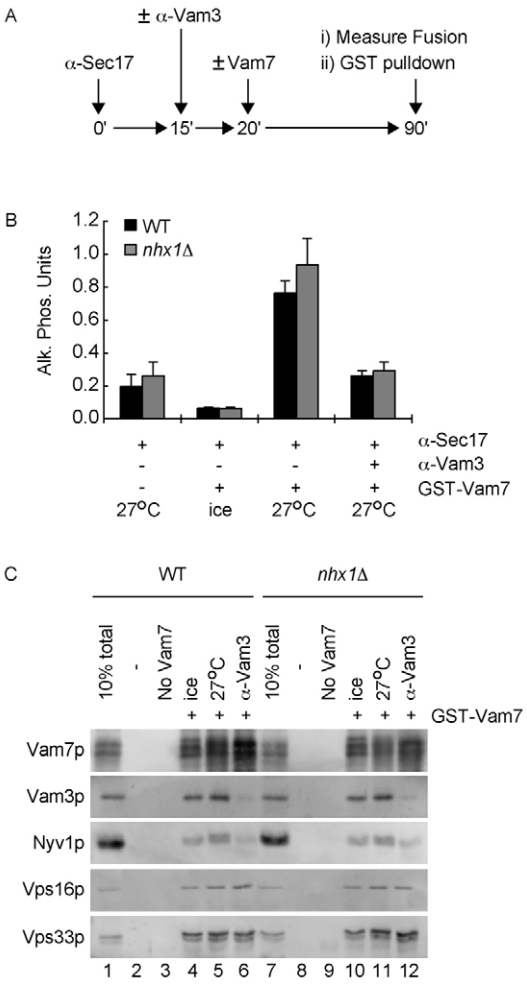

Fig. 6. Vam7p forms complexes with SNAREs and HOPS on *nhx1*Δ vacuoles. (**A**) Reaction scheme. (**B**) Large-scale fusion reactions were incubated with anti-Sec17p IgG to block priming. After 15 minutes, anti-Vam3p IgG was added to the indicated reactions and incubated for 5 minutes prior to adding 400 nM GST-Vam7p. Reactions were incubated for an additional 70 minutes. After incubation, reactions were placed on ice and 30 µl was removed to measure fusion. (**C**) The remaining fractions were extracted with solubilization buffer with protease inhibitors for 20 minutes while on ice. Insoluble debris was sedimented by centrifugation and supernatants were removed and incubated with equilibrated GSH sepharose. Beads were washed with solubilization buffer and protein complexes were eluted with SDS-PAGE buffer. Eluents were resolved by SDS-PAGE, transferred to nitrocellulose and probed with antibodies against Vam3p, Vam7p, Nyv1p, Vps16p and Vps33p. Error bars represent s.e.m. (*n*=3).

priming was blocked. However, it was unclear whether endogenous SNAREs could form trans-complexes when priming was allowed. To address this, *NHX1* was deleted from the trans-SNARE reporter strain BJ3505 CBP-Vam3p *nvy1*Δ to create RFY7. Vacuoles from RFY6 (*pho8*Δ *VAM3 NYV1*) and RFY7 were incubated together and trans-SNARE complexes were isolated through the calmodulin binding peptide (CBP) integrated into Vam3p. CBP-Vam3p complexes were isolated using calmodulin sepharose beads and resolved by SDS-PAGE. As shown in previous figures, *nhx1*Δ vacuoles were attenuated for fusion (Fig. 7A); however, the addition of excess recombinant Vam7p did not rescue fusion. Although there is a modest increase in fusion from the presence of Vam7p,

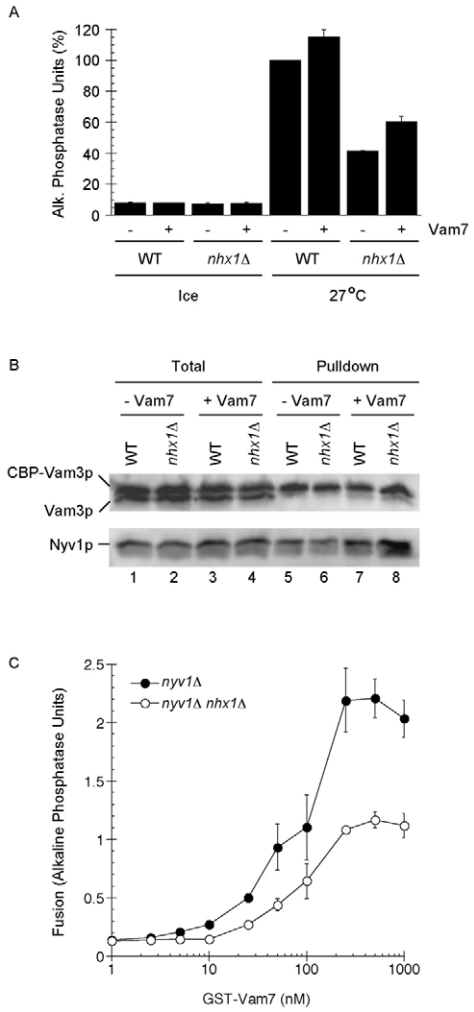

Fig. 7. Trans-SNARE complex formation. Vacuoles harboring CBP-Vam3p in a *nyv1*Δ background were incubated with vacuoles harboring a full complement of SNAREs. Large-scale reactions (16×) were incubated at 27°C for 60 minutes. After incubating, reactions were placed on ice for 5 minutes and 30 μl was withdrawn from each sample to assay Pho8p activity (**A**). The remaining samples were centrifuged and the supernatants were discarded. Membrane pellets were suspended with solubilization buffer containing protease inhibitors. (**B**) CBP-Vam3p complexes were isolated with calmodulin sepharose 4B beads, and protein complexes were resolved by SDS-PAGE and probed for Nyv1p by western blot. (**C**) Vam7p did not rescue CBP-Vam3p *nyv1*Δ *nhx1*Δ. Vacuoles from *nhx1*Δ yeast that harbored or lacked *NYV1* were blocked with anti-Sec17p antibody to inhibit priming. Reactions were incubated with increasing concentrations of recombinant Vam7p to bypass the priming block and examined for fusion. Error bars represent s.e.m. (n=3).

the *nhx1*Δ vacuoles still fused poorly. This might be attributable to the reduction in available Nyv1p, because RFY7 (but not RFY6) lacks this protein. Surprisingly, we found that *nhx1*Δ vacuoles were able to form trans-SNARE complexes as well as WT vacuoles (Fig. 7B). This suggests that *nhx1*Δ vacuoles might also be defective in fusion stages that occur downstream of trans-SNARE pairing.

Because of the possibility that the inability of Vam7p to rescue fusion in Fig. 7A was due to a shift in its K_m, we performed a dose-response assay of Vam7p using BJ3505 *nhx1*Δ or *nhx1*Δ *nyv1*Δ double deletions. These were incubated with DKY6281 *nhx1*Δ vacuoles and priming was blocked with anti-Sec17p. We found that, in the absence of Nyv1p (RFY7 vacuoles), Vam7p was unable to fully restore fusion at any concentration (Fig. 7C). In the presence of Nyv1p, Vam7p restored fusion to wild-type levels, as seen in Fig. 5A. In Fig. 7A, we performed fusion assays in the absence of a priming block, thus a better comparison would be to equate it with dose curves performed in the absence of a priming block. As seen in Fig. 5B, Vam7p does not affect fusion when priming was allowed and is in keeping with previous findings (Fratti et al., 2007).

The data thus far suggested that the deletion of *NHX1* did not affect SNARE pairing but did affect the first round of fusion. To get a better sense of the latter, we employed a real-time lipid-dequenching assay (Reese et al., 2005; Reese and Mayer, 2005). Here, vacuoles were labeled with octadecyl rhodamine (R18), which is self-quenching at high concentrations. R18 was incorporated to the outer leaflets of vacuoles to serve as a reporter system. When labeled donor vacuoles were incubated with an excess (8-fold) of unlabeled acceptor vacuoles, rhodamine dequenching occurred immediately after the first round of fusion. Fusion was initiated by adding ATP after 5 minutes of incubation and reactions were monitored for rhodamine dequenching. WT vacuoles (white circles) showed characteristic rapid dequenching whereas lipid mixing was severely inhibited in *nhx1*Δ vacuoles (white squares), further suggesting that Nhx1p regulates early kinetics of membrane fusion (Fig. 8A). Because Vam7p rescued content mixing, we next examined whether Vam7p could restore lipid mixing. When *nhx1*Δ vacuoles were incubated with 400 nM Vam7p (gray squares), lipid mixing was not only rescued, but the rate of the reaction surpassed that of untreated WT reactions. Vam7p also enhanced the rate WT lipid mixing (gray circles). Interestingly, Vam7p did not significantly enhance the V_{max} of the reactions relative to untreated WT vacuoles, suggesting that Vam7p primarily activated the first round of fusion and not ongoing rounds. Because we observed disparate effects of Vam7p that were dependent on the state of priming, we examined lipid mixing using vacuoles treated with anti-Sec17p. The addition of anti-Sec17p did not affect the basal level of fluorescence of *nhx1*Δ vacuoles (Fig. 8B). When Vam7p was added, *nhx1*Δ vacuoles were rescued and underwent accelerated lipid mixing. The initial rate of rescued fusion was similar to untreated WT. When compared with content mixing assays in Fig. 5B, the Vam7p rescue data illustrated that exogenous Vam7p bypassed the first round of fusion only, leading us to propose that once fusion was activated, subsequent rounds of fusion no longer required exogenous Vam7p.

These experiments have led us to conclude that *nhx1*Δ vacuoles are primarily attenuated at the initiation stage of the fusion cascade. To begin examining early events in membrane fusion, we examined the release of Vam7p after priming. Because Vam7p lacks a transmembrane domain, it can be separated from the membrane after it is released from the cis-SNARE complex during priming

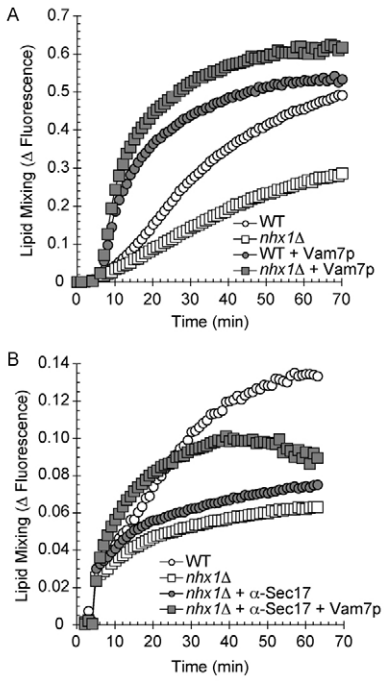

Fig. 8. Vam7p restores early fusion kinetics in *nhx1*Δ vacuoles. To measure early fusion in real time, we employed a lipid-mixing assay that measures the dequenching of octadecyl rhodamine (R18). Vacuoles were purified from yeast and labeled with R18 at self-quenching concentrations and measured for R18 dequenching. Labeled vacuoles were incubated with an 8-fold excess of unlabeled vacuoles. (**A**) WT and *nhx1*Δ vacuoles were incubated with buffer or 400 nM Vam7p. (**B**) WT and *nhx1*Δ vacuoles were treated with anti-Sec17p where indicated. Blocked vacuoles were rescued with 400 nM Vam7p. Experiments are representative of three trials.

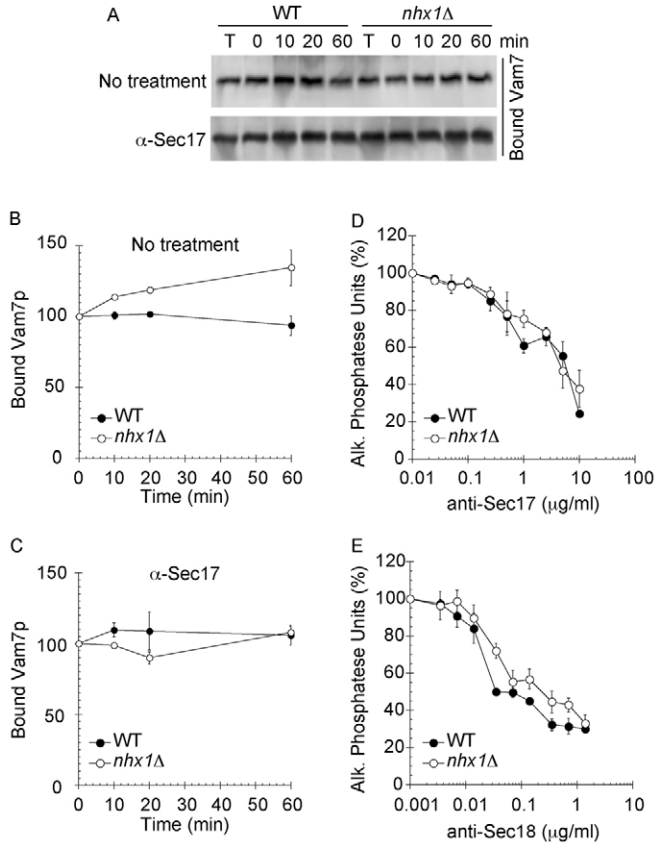

Fig. 9. Vam7p accumulates on *nhx1*Δ vacuoles. (**A**) Fusion reactions containing WT or *nhx1*Δ vacuoles treated with buffer or anti-Sec17p IgG and incubated at 27°C. At the indicated times, reactions were fractionated by centrifugation (13,000 ***g***, 15 minutes, 4°C) and supernatants were discarded. The membrane fractions were solubilized with 2× SDS loading buffer, resolved by SDS-PAGE, transferred to nitrocellulose and probed with antibody against Vam7p. (**B**,**C**) Bound Vam7p was determined by densitometry and normalized to initial (0 minutes) bound Vam7p. (**D**,**E**) Vacuoles from WT and *nhx1*Δ yeast were incubated with increasing concentrations of anti-Sec17p or anti-Sec18p and tested for fusion. Error bars represent s.e.m. (n=3).

(Boeddinghaus et al., 2002). After incubation, reactions were sedimented by centrifugation and supernatants discarded. The remaining membrane-bound Vam7p was detected by western blotting (Fig. 9A). As seen previously, WT vacuoles retain a constant level of Vam7p when reactions are uninhibited (Fig. 9B). By contrast, *nhx1*Δ vacuoles gradually accumulated Vam7p in the membrane fraction. Although this did not directly indicate that priming machinery is defective, these data do suggest that *nhx1*Δ vacuoles are altered in Vam7p binding. As a control for priming-dependent Vam7p release, we also performed parallel experiments in the presence of anti-Sec17p. Inhibiting priming prevents the release of Vam7p during incubations (Boeddinghaus et al., 2002; Fratti et al., 2004). In the presence of anti-Sec17p, both WT and *nhx1*Δ vacuoles maintained level concentrations of membrane-bound Vam7p throughout the experiment (Fig. 9C), suggesting that Vam7p accumulation on mutant vacuoles might be due to a priming defect. Any dysfunction in priming that occurred on *nhx1*Δ vacuoles was not mirrored when inhibition curves were performed using antibodies against Sec17p or Sec18p. WT and *nhx1*Δ vacuoles were incubated with increasing concentrations of anti-Sec17p (Fig. 9D) or anti-Sec18p (Fig. 9E). Although both antibodies potently blocked fusion, we did not observe a shift in sensitivity when using *nhx1*Δ vacuoles. This suggests that the priming machinery itself is not affected and that Vam7p retention on mutant vacuoles might be due to an indirect mechanism.

After priming, vacuoles undergo Ypt7p-dependent tethering that is sensitive to GAP activity. Because Nhx1p interacts with the GAP Gyp6p, which is reported to activate Ypt7p, we examined whether eliminating this interaction would influence the effectiveness of Gyp1-46p on Ypt7p (Wang et al., 2003). When WT and *nhx1*Δ vacuoles were treated with increasing concentrations of Gyp1-46, we did not observe a shift in sensitivity (Fig. 10). In keeping with these results, Ypt7p levels were not affected on mutant vacuoles (Fig. 1C). Together, these data suggest that tethering was not affected on *nhx1*Δ vacuoles.

Discussion

Nhx1p regulates the trafficking of cargo from late endosomes to the vacuole and includes the transport of the protease CPY and Vph1p, a V_0 subunit of the vacuolar V-ATPase (Bowers et al., 2000). However, the exact role of Nhx1p in regulation of the core fusion machinery had not been addressed. In this study, we showed that Nhx1p indirectly regulates early kinetics of fusion through mechanisms dependent on ion transport and lumenal pH maintenance. However, the direct effect of dysregulated pH maintenance remains unclear. Defective fusion of *nhx1*Δ vacuoles was not irreversible, as the addition of exogenous Vam7p restored

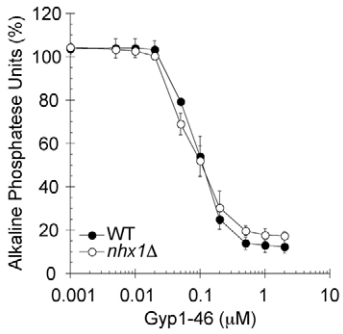

Fig. 10. Fusion inhibition by Gyp1-46p. Vacuoles from WT and *nhx1*Δ strains were incubated with increasing concentrations Gyp1-46p and tested for fusion. Error bars represent s.e.m. (n=3).

fusion to wild-type levels. Fusion was only rescued when priming was blocked with anti-Sec17p antibody. Vam7p was not able to restore fusion when priming was allowed. This was observed in both standard content mixing assays in the presence of a full complement of SNAREs, as well as trans-SNARE complex isolation experiments performed in the absence of Nyv1p on BJ3505 vacuoles. Although fusion was altered under these conditions, SNARE complex formation and SNARE-HOPS interactions were not affected on *nhx1*Δ membranes, suggesting that Nhx1p might also regulate fusion after trans-SNARE pairing. When examining the first round of fusion, as measured by lipid mixing, we found that Vam7p stimulated lipid mixing whether or not priming was blocked, indicating that Vam7p can only initiate the first round of fusion. Taken together, these data imply that Nhx1p might regulate fusion at multiple stages and that *nhx1*Δ vacuoles are defective in the initial activation of the fusion pathway, as well as post-docking events downstream of trans-SNARE complex formation.

We were able to determine by two criteria that Nhx1p regulates the initiation of the first round of fusion. Initially, we used content mixing assays that distinguish between the first round of fusion from late ongoing rounds. This approach illustrated that *nhx1*Δ vacuoles were only defective during the first round of fusion. The second measure came from a well-established lipid-mixing assay that relies on the dequenching of R18 during bilayer fusion. This experimental system utilizes an 8-fold excess of unlabeled vacuoles in the presence of R18-labeled membranes and, similar to the aforementioned content mixing assay, primarily shows the first round of fusion. Previously, this assay has been used as a measure of hemifusion that occurs between docking and full content mixing (Jun and Wickner, 2007; Reese et al., 2005; Reese and Mayer, 2005). However, we observed that *nhx1*Δ vacuoles exhibited a greater attenuation in lipid mixing relative to full content mixing. These results are inconsistent with the interpretation that lipid mixing equates with hemifusion. Currently, there is no evidence indicating that content mixing occurs without lipid mixing. Robust lipid mixing accompanies all fusion reactions, including transient reversible 'kiss-and-run' fusion (Giraudo et al., 2005). Thus, we posit that lipid-dequenching experiments report the first round of fusion and not hemifusion. This recasting reconciles our data in a manner consistent with dysfunctional early kinetics of membrane fusion.

The mechanisms by which Nhx1p directly regulates fusion remain unknown. One possibility is that fusion requires Nhx1p-dependent trafficking of Vph1p subunits to the vacuole. In the absence of Nhx1p, protein sorting to the vacuole is defective and cargo such as CPY and Vph1p are mis-sorted. Whereas CPY is secreted, Vph1p accumulates in the prevacuolar compartment, leading to dysfunctional pH maintenance, and potentially inhibits pH-independent function(s). Although Vph1p accumulates in the PVC of *nhx1*Δ cells (Bowers et al., 2000), approximately 50% reaches the vacuole (Fig. 1C). This is of particular interest because of the proposed role of the V_0 complex in homotypic fusion (Peters et al., 2001). Previous studies have suggested that the V_0 subunit of the V-ATPase is crucial for membrane fusion in yeast and other organisms (Bayer et al., 2003; Hiesinger et al., 2005; Peri and Nusslein-Volhard, 2008; Peters et al., 2001; Wassmer et al., 2005). The function of the V_0 complex in membrane fusion is independent of proton pumping and is thought to form a trans-V_0 complex that functions downstream of trans-SNARE complexes (Peters et al., 2001). Here, we found that *nhx1*Δ vacuoles, which are reduced in Vph1p, were able to fuse at WT levels when stimulated with Vam7p. This suggests that sufficient Vph1p reaches the vacuole for fusion to occur. However, this does not exclude the possibility that exogenous Vam7p (in the presence of a anti-Sec17 block) bypasses the need for full V_0 function.

Another possible regulatory target of Nhx1p is actin remodeling. Vacuole fusion requires actin remodeling at two different stages of fusion (Eitzen et al., 2002). Early fusion stages that precede docking are accompanied by the depolymerization of actin filaments. Following the docking stage, actin monomers are repolymerized prior to fusion. Although the role for actin remodeling remains unclear, inhibition of either mechanism abolishes vacuole fusion. The mammalian homolog of Nhx1p, Nhe1, is able to partially regulate actin remodeling through its interactions with Rho1, Cdc42 and ezrin (Denker et al., 2000; Frantz et al., 2007; Paradiso et al., 2004; Rasmussen et al., 2008; Wu et al., 2004). This raises the question of whether Nhx1p regulates actin remodeling during vacuole fusion. Thus far, interactions between Nhx1p and the actin network have not been explored.

Our study has revealed an unexpected role for the function of a $Na^+(K^+)/H^+$ exchanger in vacuole fusion. This is the first report to show the direct regulation of membrane fusion by a member of the NHE family. These findings add another layer to the exquisite regulation of membrane fusion and open new avenues for future investigations.

Materials and Methods

Reagents

Reagents were dissolved in PS buffer (20 mM PIPES-KOH, pH 6.8, 200 mM sorbitol). Antibodies against actin, Nyv1p, Pep4p, Pho8p, Sec17p, Sec18p, Vam3p, Vam7p, Vps11p, Vps16p, Vps33p, Vps39p and Vps41p were described previously (Haas and Wickner, 1996; Mayer and Wickner, 1997; Nichols et al., 1997; Price et al., 2000; Seals et al., 2000; Haas et al., 1995; Tedrick et al., 2004; Ungermann and Wickner, 1998). Anti-Vph1p monoclonal antibody was purchased from MitoSciences (Eugene, OR, USA). Antibodies against Vps23p and Snf7p were a gift from M. Babst (University of Utah, USA). Recombinant GST-Vam7p (wild-type and Q283R) and His6-Gyp1-46p were produced as described and dialyzed into PS buffer with 125 mM KCl (Fratti et al., 2007; Wang et al., 2003). Monoclonal anti-GST and chloroquine were from Sigma.

Strains

BJ3505 [MATα pep4::HIS3 prb1-Δ1.6R his3–200 lys2–801 trp1Δ101 (gal3) ura3–52 gal2 can1] and DKY6281 (MATα leu2–3 leu2–112 ura3–52 his3-Δ200 trp1-Δ901 lys2–801) were used for fusion assays (Haas et al., 1994) (Table 1). BJ3505 CBP-Vam3p nyv1Δ was used for trans-SNARE complex isolation (Collins and Wickner, 2007). NHX1 was deleted from BJ3505, DKY6281 and BJ3505 CBP-Vam3p nyv1Δ by homologous recombination. NHX1 was deleted with the URA3 cassette using PCR products amplified from pRS406 (Brachmann et al., 1998) with homology flanking the NHX1 coding sequence with forward primer

Table 1. Yeast strains used in this study

Strain	Genotype	Source
BJ3505	*MATα pep4::HIS3 prb1-Δ1.6R his3–200 lys2–801 trp1Δ101 (gal3) ura3–52 gal2 can1*	Jones et al., 1982
DKY6281	*MATα leu2–3 leu 2–112 ura3–52 his3-Δ200 trp1-Δ901 lys2–801*	Haas et al., 1994
BJ3505 CBP-Vam3 *nyv1Δ*	BJ3505, *CBP-VAM3::Kan^r nyv1Δ::nat^r*	Collins and Wickner, 2007
RFY5	BJ3505, *nhx1Δ::URA3*	This study
RFY6	DKY6281, *nhx1Δ::URA3*	This study
RFY7	BJ3505 CBP-*VAM3 nyv1Δ nhx1Δ::URA3*	This study
RFY8	DKY6281, *nyv1Δ nhx1Δ::URA3*	This study
RFY9	DKY6281, *NHX1::GST*	This study
RFY10	RFY5, *NHX1::3XHA*	This study
RFY11	RFY6, *NHX1::3XHA*	This study
RFY12	RFY5, *NHX1^{D201N}::3XHA*	This study
RFY13	RFY6, *NHX1^{D201N}::3XHA*	This study
RFY14	RFY5, *NHX1^{E355Q}::3XHA*	This study
RFY15	RFY6, *NHX1^{E355Q}::3XHA*	This study
RFY16	DKY6281, *NHX1::GFP*	This study

5′-GCACCCAAGATTGACAAATAGTTGTAGATTAAACATAGATAGATTGTAC-TGAGAGTGCAC-3′ and reverse primer 5′-GTATTCCTTCGGCGTTGAG-TAAGAGAGAATGTATAAAGACCTGTGCGGTATTTCACACCG-3′. The PCR product was transformed into BJ3505, DKY6281 and BJ3505 CBP-Vam3p nyv1Δ by standard lithium acetate methods and plated on complete synthetic media lacking uracil to generate BJ3505 nhx1Δ::URA3 (RFY5), DKY6281 nhx1Δ::URA3 (RFY6), BJ3505 CBP-Vam3p nyv1Δ nhx1Δ::URA3 (RFY7) and DKY6281 nyv1Δ nhx1Δ::URA3 (RFY8). For vacuole localization studies, NHXI was fused in-frame to GST or GFP by homologous recombination. DKY6281 was transformed with PCR products amplified from pFA6a-kanMX6-GST with forward primer 5′-GGCTACGCAATCACCTGCAGATTTCTCTTCCCAAAACCACCGGATCCC-CGGGTTAATTAA-3′ and reverse primer 5′-ATATTTATATTAGAAACAAG-GAAACCATACACTTTAAAGTGAATTCGAGCTCGTTTAAAC-3′ (Longtine et al., 1998) with homology flanking the stop codon of the NHX1 gene to make RFY9 (DKY6281 NHX1::GST). Similarly, DKY6281 was transformed with PCR products amplified from pFA6a-GFP(S65T)-kanMX6 with forward primer 5′-TCTCCATCCTTACAAGATTCGGCTACGCAATCACCTGCAGATTTCTCTT-CCCAAAACCACCGGATCCCCGGGTTAATTAA-3′ and reverse primer 5′-TGTATAAAGACTTAATTAATATATTTATATTAGAAACAAGGAAACCATAC-ACTTTAAAGTGAATTCGAGCTCGTTTAAAC-3′ with homology flanking the stop codon of the NHX1 gene to make RFY16 (DKY6281 NHX1::GFP). RFY5 and RFY6 were complemented with WT and mutant NHX1-HA as described (Bowers et al., 2000). WT NHX1-HA and NHX1-HA mutants (D201N and E355Q) were subcloned from the pRS316 CEN-URA3 plasmids (Bowers et al., 2000) (a gift from T. Stevens, University of Oregon, USA) into pRS413 (HIS3) and pRS414 (TRP1) using *Sal*I and *Not*I. Transformants were selected using complete synthetic media lacking His or Trp.

Vacuole isolation and in vitro vacuole fusion

Vacuoles were isolated by floatation as described (Haas et al., 1994). Standard in vitro fusion reactions (30 µl) contained 3 µg each of vacuoles from BJ3505 and DKY6281 backgrounds, fusion reaction buffer (20 mM PIPES-KOH pH 6.8, 200 mM sorbitol, 125 mM KCl, 5 mM $MgCl_2$), ATP regenerating system (1 mM ATP, 0.1 mg/ml creatine kinase, 29 mM creatine phosphate), 10 µM CoA and 283 nM IB_2. Reactions were incubated at 27°C and Pho8p activity was assayed in 250 mM Tris-Cl, pH 8.5, 0.4% Triton X-100, 10 mM $MgCl_2$, 1 mM p-nitrophenyl phosphate. Fusion units were measured by determining the p-nitrophenolate produced minute^{-1} µg^{-1} *pep4*Δ vacuole. p-nitrophenolate absorbance was detected at 400 nm.

Microsomes were prepared as described (Sorin et al., 1997). WT and *nhx1*Δ cultures were grown in YPD, washed three times with PBS and suspended in lysis buffer (10 mM Tris-CL, pH 7.4, 300 mM sorbitol, 100 mM NaCl, 5 mM $MgCl_2$) with protease inhibitors (1 mM PMSF, 10 µM Pefabloc-SC, 5 µM pepstatin A and 1 µM leupeptin). Cells were disrupted with glass beads by cycles of vortexing and cooling on ice. Lysates were centrifuged to pellet large debris and supernatants were transferred to ultracentrifuge tubes. A total membrane fraction was collected by centrifugation (100,000 ***g***, 1 hour, 4°C) and resuspended in buffer (20 mM HEPES-KOH, pH 7.4 with protease inhibitors).

GST-Vam7p SNARE complex isolation and bypass fusion

SNARE complex isolation was performed as described previously using GST-Vam7p (Fratti et al., 2007; Fratti and Wickner, 2007). Briefly, large-scale 6× fusion reactions (180 µl) were incubated with 85 µg/ml anti-Sec17p IgG to block priming. After 15 minutes, 4.3 µg/ml affinity-purified anti-Vam3p IgG was added to selected reactions and incubated for an additional 5 minutes before adding 400 nM GST-Vam7p. After a total of 90 minutes, reactions were placed on ice for 5 minutes and 30 µl aliquots were removed to measure fusion activity. The remaining 150 µl reactions were sedimented (11,000 ***g***, 10 minutes, 4°C) and the supernatants removed before extracting vacuoles with solubilization buffer (SB; 20 mM HEPES-KOH, pH 7.4, 100 mM NaCl, 2 mM EDTA, 20% glycerol, 0.5% Triton X-100, 1 mM DTT) with protease inhibitors (1 mM PMSF, 10 µM Pefabloc-SC, 5 µM pepstatin A and 1 µM leupeptin). Vacuole pellets were overlaid with 100 µl SB and resuspended gently. An additional 100 µl SB was added, gently mixed and incubated on ice for 20 minutes. Insoluble debris was sedimented (16,000 ***g***, 10 minutes, 4°C) and 176 µl of supernatants were removed and placed in chilled tubes. Next, 16 µl was removed from each reaction as 10% total samples, mixed with 8 µl of 3× SDS loading buffer and heated (95°C, 5 minutes). The remaining extracts were incubated with 30 µl equilibrated glutathione sepharose 4B beads (GE Healthcare; 15 hours, 4°C, nutating). Beads were sedimented and washed 5× with 1 ml SB (735 ***g***, 2 minutes, 4°C) and bound material was eluted with 40 µl 1× SDS loading buffer. Protein complexes were examined by western blotting. Secondary antibodies conjugated to alkaline phosphatase (Pierce) were used with ECF reagent (GE Healthcare). Images were acquired using a Storm Phosphorimager 840 (Molecular Dynamics).

Trans-SNARE complex assay

Analysis of trans-SNARE complex formation was conducted as described with some modifications (Collins and Wickner, 2007; Jun and Wickner, 2007). Complex formation was compared between reactions containing vacuoles from RFY6 and RFY7 relative to those with BJ3505-CBP-Vam3p *nyv1*Δ and DKY6281 vacuoles. The trans-SNARE assays were performed using 16× large-scale reactions (480 µl) containing 48 µg of vacuoles each from BJ3505 CBP-Vam3p *nyv1*Δ and DKY6281 backgrounds and incubated at 27°C for 60 minutes. After incubating, reactions were placed on ice for 5 minutes and 30 µl was withdrawn from each sample to assay Pho8p activity. The remaining 450 µl samples were centrifuged (13,000 ***g***, 15 minutes, 4°C) and the supernatants decanted. Vacuole pellets were overlaid with 200 µl ice-cold SB (20 mM Tris-Cl pH 7.5, 150 mM NaCl, 1 mM $MgCl_2$ 0.5% Nonidet P-40 alternative, 10% glycerol) with protease inhibitors (0.46 µg/ml leupeptin, 3.5 µg/ml pepstatin, 2.4 µg/ml pefabloc-SC, 1 mM PMSF) and gently resuspended. SB was added to a final volume of 600 µl and extracts were mixed (20 minutes, 4°C, nutating). Detergent-insoluble debris was removed by centrifugation (16,000 ***g***, 20 minutes, 4°C). Supernatants were transferred to fresh tubes and 10% of the extract was removed for input samples. The remaining extracts were brought to 2 mM $CaCl_2$. CBP-Vam3p complexes were incubated with 50 µl equilibrated calmodulin sepharose 4B (GE Healthcare; 4°C, 12 hours, nutating). Beads were collected by centrifugation (4000 ***g***, 2 minutes, 4°C) and suspended four times with the SB, followed by bead sedimentation. Bound proteins were eluted with SDS sample buffer containing 5 mM EGTA and heated at 95°C for 5 minutes. The samples were used for SDS-PAGE analysis and immunoblotting.

Lipid mixing

Lipid mixing assays were conducted using octadecyl rhodamine B (R18; Invitrogen) as described with minor modifications (Jun and Wickner, 2007). Briefly, BJ3505 background vacuoles (300 µg) were incubated in 400 µl of PS buffer containing 150 µM R18 (10 minutes, 4°C, nutating). Samples were mixed with 15% Ficoll in PS buffer (wt/vol) and transferred to a polyallomer tube (11 × 60 mm). Samples were overlaid with 1.0 ml each of 8%, 4% and 0% Ficoll. Labeled vacuoles were re-isolated by centrifugation using a SW60 Ti rotor (105,200 ***g***, 30 minutes, 4°C) and recovered from the 0–4% Ficoll interface. Lipid mixing assays (90 µl) contained 2 µg of R18-labeled vacuoles and 16 µg of unlabeled vacuoles in fusion buffer. Reaction mixtures were transferred to a black, half-volume 96-well flat-bottom microtiter plate with nonbinding surface (Corning). Rhodamine fluorescence (λ_{ex}=544 nm; λ_{em}=590 nm) was measured using a POLARstar Omega plate reader (BMG Labtech) at 27°C. Measurements were taken every minute for 75 minutes, yielding fluorescence values at the onset (F_0) and during the reaction (F_t). The final ten measurements of a sample after adding 0.33% (vol/vol) Triton X-100 were averaged and used as a value for the fluorescence after infinite dilution (F_{TX100}). The relative total fluorescence change $\Delta F_t/F_{TX100}=(F_t-F_0)/F_{TX100}$ was calculated.

Microscopy

Vacuole morphology was monitored by incubating yeast cells with YPD (yeast-peptone-dextrose) broth containing 5 μM FM4-64. Cultures were grown overnight, washed with PS buffer, concentrated by centrifugation, mixed with 0.6% agarose and mounted on glass slides for observation. Images were acquired using a Zeiss Axio Observer Z1 inverted microscope equipped with an X-Cite 120XL light source, Plan Apochromat 63× oil objective (NA 1.4) and an AxioCam CCD camera. FM4-64 images were acquired using a 43 HE CY 3 shift-free filter set. Image deconvolution of *z*-stack images was performed using the AxioVison 3D deconvolution software module and fast iterative algorithm.

We thank Tom Stevens for *NHX1* plasmids, and William Wickner and Markus Babst for generous gifts of antisera. We also thank Kevin Collins, Vincent Starai, Robert Switzer, Emad Tajkhorshid and members of the Fratti laboratory for helpful discussions. This work was supported by startup funds provided to R.A.F. by the University of Illinois at Urbana-Champaign.

References

Aharonovitz, O., Zaun, H. C., Balla, T., York, J. D., Orlowski, J. and Grinstein, S. (2000). Intracellular pH regulation by Na^+/H^+ exchange requires phosphatidylinositol 4,5-bisphosphate. *J. Cell Biol.* **150**, 213-224.

Ali, R., Brett, C. L., Mukherjee, S. and Rao, R. (2004). Inhibition of sodium/proton exchange by a Rab-GTPase-activating protein regulates endosomal traffic in yeast. *J. Biol. Chem.* **279**, 4498-4506.

Babst, M., Katzmann, D. J., Estepa-Sabal, E. J., Meerloo, T. and Emr, S. D. (2002). Escrt-III: an endosome-associated heterooligomeric protein complex required for mvb sorting. *Dev. Cell* **3**, 271-282.

Bayer, M. J., Reese, C., Buhler, S., Peters, C. and Mayer, A. (2003). Vacuole membrane fusion: V0 functions after trans-SNARE pairing and is coupled to the Ca^{2+}-releasing channel. *J. Cell Biol.* **162**, 211-222.

Boeddinghaus, C., Merz, A. J., Laage, R. and Ungermann, C. (2002). A cycle of Vam7p release from and PtdIns 3-P-dependent rebinding to the yeast vacuole is required for homotypic vacuole fusion. *J. Cell Biol.* **157**, 79-89.

Bonangelino, C. J., Chavez, E. M. and Bonifacino, J. S. (2002). Genomic screen for vacuolar protein sorting genes in Saccharomyces cerevisiae. *Mol. Biol. Cell* **13**, 2486-2501.

Bowers, K., Levi, B. P., Patel, F. I. and Stevens, T. H. (2000). The sodium/proton exchanger Nhx1p is required for endosomal protein trafficking in the yeast Saccharomyces cerevisiae. *Mol. Biol. Cell* **11**, 4277-4294.

Brachmann, C. B., Davies, A., Cost, G. J., Caputo, E., Li, J., Hieter, P. and Boeke, J. D. (1998). Designer deletion strains derived from Saccharomyces cerevisiae S288C: a useful set of strains and plasmids for PCR-mediated gene disruption and other applications. *Yeast* **14**, 115-132.

Brett, C. L., Tukaye, D. N., Mukherjee, S. and Rao, R. (2005). The yeast endosomal Na^+K^+/H^+ exchanger Nhx1 regulates cellular pH to control vesicle trafficking. *Mol. Biol. Cell* **16**, 1396-1405.

Collins, K. M. and Wickner, W. T. (2007). Trans-SNARE complex assembly and yeast vacuole membrane fusion. *Proc. Natl. Acad. Sci. USA* **104**, 8755-8760.

Denker, S. P., Huang, D. C., Orlowski, J., Furthmayr, H. and Barber, D. L. (2000). Direct binding of the Na-H exchanger NHE1 to ERM proteins regulates the cortical cytoskeleton and cell shape independently of H^+ translocation. *Mol. Cell* **6**, 1425-1436.

Dibrov, P., Young, P. G. and Fliegel, L. (1998). Functional analysis of amino acid residues essential for activity in the Na^+/H^+ exchanger of fission yeast. *Biochemistry* **37**, 8282-8288.

Eitzen, G., Wang, L., Thorngren, N. and Wickner, W. (2002). Vacuole-bound actin regulates homotypic membrane fusion. *J. Cell Biol.* **158**, 669-679.

Fafournoux, P., Noel, J. and Pouyssegur, J. (1994). Evidence that Na+/H+ exchanger isoforms NHE1 and NHE3 exist as stable dimers in membranes with a high degree of specificity for homodimers. *J. Biol. Chem.* **269**, 2589-2596.

Frantz, C., Karydis, A., Nalbant, P., Hahn, K. M. and Barber, D. L. (2007). Positive feedback between Cdc42 activity and H^+ efflux by the Na-H exchanger NHE1 for polarity of migrating cells. *J. Cell Biol.* **179**, 403-410.

Fratti, R. A. and Wickner, W. (2007). Distinct targeting and fusion functions of the PX and SNARE domains of yeast vacuolar Vam7p. *J. Biol. Chem.* **282**, 13133-13138.

Fratti, R. A., Jun, Y., Merz, A. J., Margolis, N. and Wickner, W. (2004). Interdependent assembly of specific regulatory lipids and membrane fusion proteins into the vertex ring domain of docked vacuoles. *J. Cell Biol.* **167**, 1087-1098.

Fratti, R. A., Collins, K. M., Hickey, C. M. and Wickner, W. (2007). Stringent 3Q: 1R composition of the SNARE 0-layer can be bypassed for fusion by compensatory SNARE mutation or by lipid bilayer modification. *J. Biol. Chem.* **282**, 14861-14867.

Giraudo, C. G., Hu, C., You, D., Slovic, A. M., Mosharov, E. V., Sulzer, D., Melia, T. J. and Rothman, J. E. (2005). SNAREs can promote complete fusion and hemifusion as alternative outcomes. *J. Cell Biol.* **170**, 249-260.

Haas, A. and Wickner, W. (1996). Homotypic vacuole fusion requires Sec17p (yeast alpha-SNAP) and Sec18p (yeast NSF). *EMBO J.* **15**, 3296-3305.

Haas, A., Conradt, B. and Wickner, W. (1994). G-protein ligands inhibit in vitro reactions of vacuole inheritance. *J. Cell Biol.* **126**, 87-97.

Haas, A., Scheglmann, D., Lazar, T., Gallwitz, D. and Wickner, W. (1995). The GTPase Ypt7p of Saccharomyces cerevisiae is required on both partner vacuoles for the homotypic fusion step of vacuole inheritance. *EMBO J.* **14**, 5258-5270.

Hiesinger, P. R., Fayyazuddin, A., Mehta, S. Q., Rosenmund, T., Schulze, K. L., Zhai, R. G., Verstreken, P., Cao, Y., Zhou, Y., Kunz, J. et al. (2005). The v-ATPase V0 subunit a1 is required for a late step in synaptic vesicle exocytosis in Drosophila. *Cell* **121**, 607-620.

Inoue, H., Noumi, T., Tsuchiya, T. and Kanazawa, H. (1995). Essential aspartic acid residues, Asp-133, Asp-163 and Asp-164, in the transmembrane helices of a Na+/H+ antiporter (NhaA) from Escherichia coli. *FEBS Lett.* **363**, 264-268.

Isgandarova, S., Jones, L., Forsberg, D., Loncar, A., Dawson, J., Tedrick, K. and Eitzen, G. (2007). Stimulation of actin polymerization by vacuoles via Cdc42p-dependent signaling. *J. Biol. Chem.* **282**, 30466-30475.

Jahn, R. and Sudhof, T. C. (1999). Membrane fusion and exocytosis. *Annu. Rev. Biochem.* **68**, 863-911.

Jones, E. W., Zubenko, G. S. and Parker, R. R. (1982). PEP4 gene function is required for expression of several vacuolar hydrolases in *Saccharomyces cerevisiae*. *Genetics* **102**, 665-677.

Jun, Y. and Wickner, W. (2007). Assays of vacuole fusion resolve the stages of docking, lipid mixing, and content mixing. *Proc. Natl. Acad. Sci. USA* **104**, 13010-13015.

Jun, Y., Fratti, R. A. and Wickner, W. (2004). Diacylglycerol and its formation by Phospholipase C regulate Rab- and SNARE-dependent yeast vacuole fusion. *J. Biol. Chem.* **279**, 53186-53195.

Kato, M. and Wickner, W. (2001). Ergosterol is required for the Sec18/ATP-dependent priming step of homotypic vacuole fusion. *EMBO J.* **20**, 4035-4040.

Katzmann, D. J., Babst, M. and Emr, S. D. (2001). Ubiquitin-dependent sorting into the multivesicular body pathway requires the function of a conserved endosomal protein sorting complex, ESCRT-I. *Cell* **106**, 145-155.

Longtine, M. S., McKenzie, A., 3rd, Demarini, D. J., Shah, N. G., Wach, A., Brachat, A., Philippsen, P. and Pringle, J. R. (1998). Additional modules for versatile and economical PCR-based gene deletion and modification in Saccharomyces cerevisiae. *Yeast* **14**, 953-961.

Mayer, A. and Wickner, W. (1997). Docking of yeast vacuoles is catalyzed by the Ras-like GTPase Ypt7p after symmetric priming by Sec18p (NSF). *J. Cell Biol.* **136**, 307-317.

Mayer, A., Wickner, W. and Haas, A. (1996). Sec18p (NSF)-driven release of Sec17p (alpha-SNAP) can precede docking and fusion of yeast vacuoles. *Cell* **85**, 83-94.

Merz, A. J. and Wickner, W. (2004a). *Trans*-SNARE interactions elicit Ca^{2+} efflux from the yeast vacuole lumen. *J. Cell Biol.* **164**, 195-206.

Merz, A. J. and Wickner, W. T. (2004b). Resolution of organelle docking and fusion kinetics in a cell-free assay. *Proc. Natl. Acad. Sci. USA* **101**, 11548-11553.

Mukherjee, S., Kallay, L., Brett, C. L. and Rao, R. (2006). Mutational analysis of the intramembranous H10 loop of yeast Nhx1 reveals a critical role in ion homoeostasis and vesicle trafficking. *Biochem. J.* **398**, 97-105.

Nass, R. and Rao, R. (1998). Novel localization of a Na^+/H^+ exchanger in a late endosomal compartment of yeast. Implications for vacuole biogenesis. *J. Biol. Chem.* **273**, 21054-21060.

Nichols, B. J., Ungermann, C., Pelham, H. R., Wickner, W. T. and Haas, A. (1997). Homotypic vacuolar fusion mediated by t- and v-SNAREs. *Nature* **387**, 199-202.

Paradiso, A., Cardone, R. A., Bellizzi, A., Bagorda, A., Guerra, L., Tommasino, M., Casavola, V. and Reshkin, S. J. (2004). The Na^+-H^+ exchanger-1 induces cytoskeletal changes involving reciprocal RhoA and Rac1 signaling, resulting in motility and invasion in MDA-MB-435 cells. *Breast Cancer Res.* **6**, R616-R628.

Peri, F. and Nusslein-Volhard, C. (2008). Live imaging of neuronal degradation by microglia reveals a role for v0-ATPase a1 in phagosomal fusion in vivo. *Cell* **133**, 916-927.

Peters, C., Bayer, M. J., Buhler, S., Andersen, J. S., Mann, M. and Mayer, A. (2001). Trans-complex formation by proteolipid channels in the terminal phase of membrane fusion. *Nature* **409**, 581-588.

Price, A., Seals, D., Wickner, W. and Ungermann, C. (2000). The docking stage of yeast vacuole fusion requires the transfer of proteins from a cis-SNARE complex to a Rab/Ypt protein. *J. Cell Biol.* **148**, 1231-1238.

Rasmussen, M., Alexander, R. T., Darborg, B. V., Mobjerg, N., Hoffmann, E. K., Kapus, A. and Pedersen, S. F. (2008). Osmotic cell shrinkage activates ezrin/radixin/moesin (ERM) proteins: activation mechanisms and physiological implications. *Am. J. Physiol. Cell Physiol.* **294**, C197-C212.

Reese, C. and Mayer, A. (2005). Transition from hemifusion to pore opening is rate limiting for vacuole membrane fusion. *J. Cell Biol.* **171**, 981-990.

Reese, C., Heise, F. and Mayer, A. (2005). Trans-SNARE pairing can precede a hemifusion intermediate in intracellular membrane fusion. *Nature* **436**, 410-414.

Seals, D. F., Eitzen, G., Margolis, N., Wickner, W. T. and Price, A. (2000). A Ypt/Rab effector complex containing the Sec1 homolog Vps33p is required for homotypic vacuole fusion. *Proc. Natl. Acad. Sci. USA* **97**, 9402-9407.

Seeley, E. S., Kato, M., Morgolis, N., Wickner, W. and Eitzen, G. (2002). Genomic analysis of homotypic vacuole fusion. *Mol. Biol. Cell* **13**, 782-794.

Sorin, A., Rosas, G. and Rao, R. (1997). PMR1, a Ca2+-ATPase in yeast Golgi, has properties distinct from sarco/endoplasmic reticulum and plasma membrane calcium pumps. *J. Biol. Chem.* **272**, 9895-9901.

Stroupe, C., Collins, K. M., Fratti, R. A. and Wickner, W. (2006). Purification of active HOPS complex reveals its affinities for phosphoinositides and the SNARE Vam7p. *EMBO J.* **25**, 1579-1589.

Tedrick, K., Trischuk, T., Lehner, R. and Eitzen, G. (2004). Enhanced membrane fusion in sterol-enriched vacuoles bypasses the Vrp1p requirement. *Mol. Biol. Cell* **15**, 4609-4621.

Thorngren, N., Collins, K. M., Fratti, R. A., Wickner, W. and Merz, A. J. (2004). A soluble SNARE drives rapid docking, bypassing ATP and Sec17/18p for vacuole fusion. *EMBO J.* **23**, 2765-2776.

Ungermann, C. and Wickner, W. (1998). Vam7p, a vacuolar SNAP-25 homolog, is required for SNARE complex integrity and vacuole docking and fusion. *EMBO J.* **17**, 3269-3276.

Ungermann, C., Sato, K. and Wickner, W. (1998). Defining the functions of trans-SNARE pairs. *Nature* **396**, 543-548.

Vida, T. A. and Emr, S. D. (1995). A new vital stain for visualizing vacuolar membrane dynamics and endocytosis in yeast. *J. Cell Biol.* **128**, 779-792.

Wang, L., Seeley, E. S., Wickner, W. and Merz, A. J. (2002). Vacuole fusion at a ring of vertex docking sites leaves membrane fragments within the organelle. *Cell* **108**, 357-369.

Wang, L., Merz, A. J., Collins, K. M. and Wickner, W. (2003). Hierarchy of protein assembly at the vertex ring domain for yeast vacuole docking and fusion. *J. Cell Biol.* **160**, 365-374.

Wassmer, T., Froissard, M., Plattner, H., Kissmehl, R. and Cohen, J. (2005). The vacuolar proton-ATPase plays a major role in several membrane-bounded organelles in *Paramecium*. *J. Cell Sci.* **118**, 2813-2825.

Wells, K. M. and Rao, R. (2001). The yeast Na^+/H^+ exchanger Nhx1 is an N-linked glycoprotein. Topological implications. *J. Biol. Chem.* **276**, 3401-3407.

Will, E. and Gallwitz, D. (2001). Biochemical characterization of Gyp6p, a Ypt/Rab-specific GTPase-activating protein from yeast. *J. Biol. Chem.* **276**, 12135-12139.

Wu, K. L., Khan, S., Lakhe-Reddy, S., Jarad, G., Mukherjee, A., Obejero-Paz, C. A., Konieczkowski, M., Sedor, J. R. and Schelling, J. R. (2004). The NHE1 Na^+/H^+ exchanger recruits ezrin/radixin/moesin proteins to regulate Akt-dependent cell survival. *J. Biol. Chem.* **279**, 26280-26286.

Yamaguchi, T., Aharon, G. S., Sottosanto, J. B. and Blumwald, E. (2005). Vacuolar Na^+/H^+ antiporter cation selectivity is regulated by calmodulin from within the vacuole in a Ca^{2+}- and pH-dependent manner. *Proc. Natl. Acad. Sci. USA* **102**, 16107-16112.